

Physical properties of $\text{Bi}_2\text{Sr}_2\text{Ca}_{n-1}\text{Cu}_n\text{O}_y$ ($n = 1, 2, 3$)

A. Maeda, M. Hase, I. Tsukada, K. Noda, S. Takebayashi, and K. Uchinokura

Department of Applied Physics, The University of Tokyo, 7-3-1 Hongo, Bunkyo-ku, Tokyo 113, Japan

(Received 18 September 1989)

Polycrystalline samples of $\text{Bi}_2\text{Sr}_2\text{Ca}_{n-1}\text{Cu}_n\text{O}_y$ with various hole concentrations were synthesized by substituting La for Sr, Y for Ca, and Pb for Bi. The superconducting properties, magnetic susceptibilities, Hall coefficients, and infrared optical reflection spectra were measured after sufficient characterization of the samples. For the $n=1$ (2:2:0:1) materials, the antiferromagnetic semiconductor–superconductor–normal-metal transition was observed with increasing hole concentration. In $n=1$ materials the Hall coefficient deviates strongly from the inverse of the hole concentration with increasing hole concentration. On the other hand, in the $n=2$ (2:2:1:2) materials the Hall coefficient roughly scales with the inverse of hole concentration even for the samples exhibiting superconductivity above liquid-nitrogen temperature. The edge structure in the infrared reflection spectra shifts to higher frequencies with increasing n , whereas it did not change at all when the hole concentration was varied within the same structure (n value). Together with the result of the magnetic-susceptibility measurement, these results are discussed in terms of the several models describing the normal state of high- T_c oxide superconductors.

I. INTRODUCTION

Since the discovery by Bednorz and Muller,¹ a number of high-temperature superconductors based on copper oxide have been discovered. All of these contain the square network of the planes composed of copper and oxygen.² Empirically, the superconducting transition temperature T_c becomes higher with an increasing number of CuO_2 layers up to three. Recently, attention has been focused on the preparation and the physical properties of the materials with a larger number of CuO_2 layers.

The Bi-Sr-Ca-Cu-O (Refs. 3–5) and the Tl-Ba-Ca-Cu-O system^{6,7} form a series of compounds, $\text{Bi}_2\text{Sr}_2\text{Ca}_{n-1}\text{Cu}_n\text{O}_y$ ($n = 1, 2, 3, \dots$) and $\text{Tl}_2\text{Ba}_2\text{Ca}_{n-1}\text{Cu}_n$ ($n = 1, 2, 3, \dots$), respectively. Hereafter, we denote $n = 1, 2, 3$ materials as the 2:2:0:1, 2:2:1:2, and 2:2:2:3 materials, respectively. These compounds have crystal structures based on the stacking of Bi (or Tl)₂O₂Sr (or Ba)O-(CuO₂-CaO₂)_n-Cu-Bi (or Tl)₂O₂.^{8–10} The superconducting transition temperature T_c increases with an increasing number of CuO_2 as n increases to 3, and decreases for further increases of n .¹¹ Thus, it is interesting to investigate the change in normal-state properties when n is changed. However, even with the same n structure, various properties strongly depend on the carrier concentration. In general, it is well established that the superconducting transition temperature T_c strongly depends on the carrier concentration.² In the (La,Sr)₂-CuO₄ system which has a single CuO_2 square network, it has been known that the system becomes superconducting from the antiferromagnetic insulator with increasing hole concentration. With further increasing hole concentration, it becomes similar to a normal metal, and superconductivity disappears.¹² In the so-called 1:2:3 compounds which have a double layer of the CuO_2 square

network, saturation of the increase in T_c was also found.¹³ However, the disappearance of superconductivity with heavy doping of the hole has not yet been found.

The electronic-structure, normal-state properties also change with increasing hole concentration. One of the most striking results is the Hall effect in these materials. For instance, in the case of the (La,Sr)-Cu-O system, the Hall coefficient R_H is positive, and decreases with increasing hole concentration.^{14,15} These can be interpreted as hole doping into the Mott-Hubbard split band. (Here we use the term Mott-Hubbard splitting in the extended sense including the charge-transfer splitting.)¹⁵ In the lightly doped region, R_H roughly scales with the inverse of the hole concentration, which is consistent with the above picture. However, it strongly deviates from the inverse of the hole concentration with further increasing hole concentration, which strongly suggests that the electronic structure is altered by the hole doping. Thus, it can be said that the appearance of superconductivity may correspond to the change in the electronic structure near the Fermi surface. On the other hand, in the 1:2:3 compounds, R_H exactly scales with the inverse of hole concentration even at the hole concentration where superconductivity with $T_c = 90$ K occurs.¹⁶ Thus, in the 1:2:3 compounds, the Mott-Hubbard split-band picture seems to survive well even at the high hole-concentration region. It is a natural question whether this difference in the relation between hole concentration and R_H between the 2:1:4 and the 1:2:3 compounds is observed in other systems or not. In this sense, the Bi compounds seem to be appropriate because the crystal structure is almost the same except for the number of CuO_2 sheets.

Another interesting problem is the infrared reflection spectra of these materials. It is well known that the Drudelike reflection spectra are observed in the infrared region for a wide range of materials of high- T_c oxides.² Tajima *et al.*¹⁷ proposed an empirical relation between

the transition temperature and the “plasma frequency.” If this structure truly represents the plasma reflection, high- T_c oxides look like ordinary metals in the energy scale of infrared light, which is in sharp contrast to the Mott-Hubbard picture in dc transport properties. However, there are some puzzling experimental results. In the (La,Sr)-Cu-O system, it has been found that the “plasma frequency” does not change with increasing hole concentration, thus increasing T_c .^{17,18} On the other hand, the relaxation time τ was found to increase with increasing hole concentration. In ordinary Fermi-liquid theory, plasma frequency should be proportional to the square root of the ratio of the carrier concentration to the effective mass. Thus, the pinning of the plasma frequency observed in the (La,Sr)-Cu-O system contradicts the simple Fermi-liquid picture. Furthermore, in the low-energy region, the temperature-dependent deviation from the Drude-type behavior was reported.¹⁹ These results strongly suggest that the optical reflection spectra should be reinterpreted from a point of view quite different from the simple Drude picture. Thus, it is necessary to investigate the optical reflection spectra in other systems. In particular, as a first step, the Drudelike structure should be investigated in samples with various carrier concentrations in other systems. Again, the Bi compounds are appropriate in this sense.

In the Bi compounds, several authors reported that the control of the hole concentration is possible by substitution of cations with different chemical valence.^{20–26} In this paper, we studied the synthesis of good polycrystalline samples with various hole concentration for various n , and investigated the resistivity, the Hall effect, the infrared reflection spectra, and also the magnetic susceptibility in normal state. These results are discussed in terms of the several models describing the normal state of high- T_c oxide superconductors.

Part of the results were already published in the form of short communications.^{27–30}

II. EXPERIMENTS

Samples were prepared by an ordinary solid-state reaction method. Nearly stoichiometric amounts of Bi_2O_3 , SrCO_3 , CaCO_3 , Y_2O_3 , La_2O_3 , Pb_3O_4 , and CuO powders

were mixed with agate mortar and pestle, calcined at 830°C for 20 h. The calcined powders were pressed into pellets, and sintered at 850°C–890°C in air except for the 2:2:2:3 ($n = 3$) material. The exact nominal composition and temperature of the sintering depend on the materials. For example, we found that the single phase of the 2:2:1:2 material can be synthesized from the nominal composition of $[\text{Bi}]:[\text{Sr}]:[\text{Ca}]:[\text{Cu}] = 2:1.8:1.2:2$ rather than 2:2:1:2.²⁷ The conditions of the preparation are summarized in Table I. For the 2:2:0:1 material doped with La, we tried both $\text{Bi}_2\text{Sr}_{2-w}\text{La}_w\text{CuO}_y$ and $\text{Bi}_{2.1}\text{Sr}_{1.9-z}\text{La}_z\text{CuO}_y$ because an almost single-phase sample was obtained for $\text{Bi}_{2.1}\text{Sr}_{1.9}\text{CuO}_y$, not for $\text{Bi}_2\text{Sr}_2\text{CuO}_y$ as will be described in Sec. III A. We also synthesized Nd-doped 2:2:0:1 samples (not shown in Table I) in order to check whether superconductivity is due to 2:1:4 (La,Sr)-Cu-O or not.

It should be noted that an additional process is necessary for the preparation of good 2:2:2:3 samples.²⁸ It is well known that the introduction of Pb (Ref. 31) and the long-time sintering under low oxygen partial pressure³² remarkably improves the quality of the 2:2:2:3 sample. Our method of the preparation is basically the same as those presented in Refs. 31 and 32. However, even by this method the density of the obtained single-phase crystal is almost half the ideal value owing to the volume expansion during the sintering process.³³ Thus, further heat treatment was necessary to obtain high-quality polycrystalline samples appropriate for the physical measurement. Details were published elsewhere.²⁸

Prepared samples were characterized by ordinary powder x-ray-diffraction, dc magnetic susceptibility using a SQUID magnetometer, and dc resistivity measurements. The powder x-ray-diffraction pattern for Cu $K\alpha$ radiation was measured by a Rigaku RAD-IA powder diffractometer. For several samples, scanning electron microscopy (SEM) images were taken with a JEOL JXA-8621, together with the EPMA measurement. Thermogravimetric analysis was performed by a MAC science TG-DTA-2000.

The average valence of Cu was determined by an ordinary iodometric titration method. It is generally said that Bi and Pb take the mixed-valence state in oxide materials, which may cause experimental errors in the deter-

TABLE I. Conditions of preparation of the samples. All samples were calcined at 830°C for 20 h in air. For samples in series G (2:2:2:3 material), additional heat treatment described in the text was made.

Number of CuO_2 layers	Name of Series	Nominal composition	Sintering		
			Temperature (°C)	Time (h)	Atmosphere
1	A	$\text{Bi}_{2+x}\text{Sr}_{2-x}\text{CuO}_y$ ($-0.2 \leq x \leq 0.3$)	850	15	air
	B	$\text{Bi}_{2.1}\text{Sr}_{1.9-z}\text{La}_z\text{CuO}_y$ ($0 \leq z \leq 1$)	850	15	air
	C	$\text{Bi}_2\text{Sr}_{2-w}\text{La}_w\text{CuO}_y$ ($0 \leq w \leq 1$)	850 ($0 \leq w \leq 0.6$) 860 ($0.7 \leq w \leq 1.0$)	15	air
	D	$\text{Bi}_{2.1-x}\text{Pb}_x\text{Sr}_{1.9}\text{CuO}_y$ ($0 \leq x \leq 0.6$)	850	15	air
2	E	$\text{Bi}_2\text{Sr}_{1.8}(\text{Ca}_{1-x}\text{Y}_x)_{1.2}\text{Cu}_2\text{O}_y$ ($0 \leq x \leq 1$)	865 ($0 \leq x \leq 0.45$)	12	air
			870 ($0 \leq x \leq 0.7$)		
			880 ($0.8 \leq x \leq 0.9$)		
			890 ($x = 1.0$)		
	F	$(\text{Bi}_{1-z}\text{Pb}_z)_2\text{Sr}_{1.8}\text{Ca}_{1.2}\text{Cu}_2\text{O}_y$ ($0 \leq z \leq 0.5$)	860	12	air
3	G	$\text{Bi}_{1.85}\text{Pb}_{0.35}(\text{Sr}_{1-x}\text{Ca}_x)_4\text{Cu}_{3.1}\text{O}_y$ ($0 \leq x \leq 1$)	860–870	50–100	N_2

mination of the average valence of Cu. However, the simple assumption of Bi^{3+} gave relatively good agreement with the analyzed oxygen content.⁸ Thus, we will simply assume that Bi and Pb are trivalent and divalent, respectively. As will be described in Sec. III B 4, we can regard the deviation of the average valence of Cu from 2.0 as the hole concentration.

Magnetic susceptibility was measured by a SHE model 905 SQUID magnetometer. The susceptibility in the superconducting state (Meissner effect) and that in the normal state was measured under the magnetic field of 10 and 5 kOe, respectively. An ac magnetic susceptibility measurement was sometimes performed for the characterization of grain boundaries.

Resistivity measurement was accomplished by utilizing an ordinary four-probe method for pellets that were cut into "bar shapes". The typical dimension of the samples was $1 \times 1 \times 6 \text{ mm}^3$. Electric contacts were made using Dupont silver paste No. 6500. The contact resistance was typically 0.1Ω .

The Hall coefficient measurement was measured under the magnetic field of 1.8 T. The current was fixed at 20–50 mA depending on samples. Typical thickness of the samples was 0.1–0.2 mm.

Infrared optical reflection spectra were measured by a Parkin Elmer E1 monochromator in the frequency range between 4000 and 15000 cm^{-1} . For optical measurement in polycrystals, the method of polishing is important in order to obtain good results. We found that the following procedure provides the polycrystalline sample with high reflectivity in a well-reproducible way: First, a pellet is polished by ordinary No. 6000 Al_2O_3 powders; next, the pellet is polished by finer Al_2O_3 powders with a diameter of $0.3 \mu\text{m}$ without any liquid. Only after polishing for approximately 10 min is a mirrorlike pellet obtained. The second polishing with some liquid is much less effective.

III. EXPERIMENTAL RESULTS

A. Characterization of the samples

Figure 1 shows typical examples of the powder x-ray-diffraction patterns of the $n = 1, 2, 3$ materials. For the $n = 1$ material, single-phase samples were obtained for $0.1 \leq x \leq 0.4$ of $\text{Bi}_{2+x}\text{Sr}_{2-x}\text{CuO}_y$ (series A), $0.2 \leq w \leq 1.0$ in La-doped samples (series C), and for $0.05 \leq x \leq 0.5$ in Pb-doped samples (series D). (See Table I for nominal composition of each series.) All peaks except for Pb-doped 2:2:0:1 samples with $x > 0.1$ and Y-doped 2:2:1:2 samples with $x \geq 0.6$ were indexed by a tetragonal unit cell. The obtained lattice parameters for the 2:2:0:1 samples (series B, C, and D) are shown in Fig. 2. As was already reported in a short communication,³⁰ in Pb-doped samples with x larger than 0.1, peaks cannot be indexed by a tetragonal cell but were indexed by an orthorhombic unit cell. In the orthorhombic region, the high-resolution electron-diffraction measurement shows that the superstructure in the Bi_2O_2 plane disappears.³⁴ In the case of La-doped samples, the c parameter does not change so much for a low concentration of La, whereas the a parameter increases with increasing La content. For large

La concentration, the c parameter decreases with increasing La content. For Pb-doped samples, the c parameter does not depend on the Pb content. At the same time, with increasing Pb content the system undergoes a tetragonal to orthorhombic transition, as was described previously.

The SEM-EPMA observation of these samples shows that all parts of the sample are in the Bi 2:2:0:1 phase, with a very small amount of CuO present (2% in the area of the photograph). Thus, it can be concluded that doped ions are substituted.

It also should be noted that in the nondoped sample ($\text{Bi}_2\text{Sr}_2\text{CuO}_y$) many other phases were contained, which are easily observed in a powder x-ray-diffraction pattern. This is probably due to the existence of a $\text{Bi}_{17}\text{Sr}_{16}\text{Cu}_7\text{O}_y$ phase.³⁵ However, a single-phase solid solution can be formed by changing the ratio of Bi to Sr. Figure 3 shows the lattice parameters of $\text{Bi}_{2+x}\text{Sr}_{2-x}\text{CuO}_y$ obtained by the method of least squares. With increasing Bi content, a parameter increases without emergence of any other phases, which shows that the solid solution is surely formed with substituting Sr for Bi.

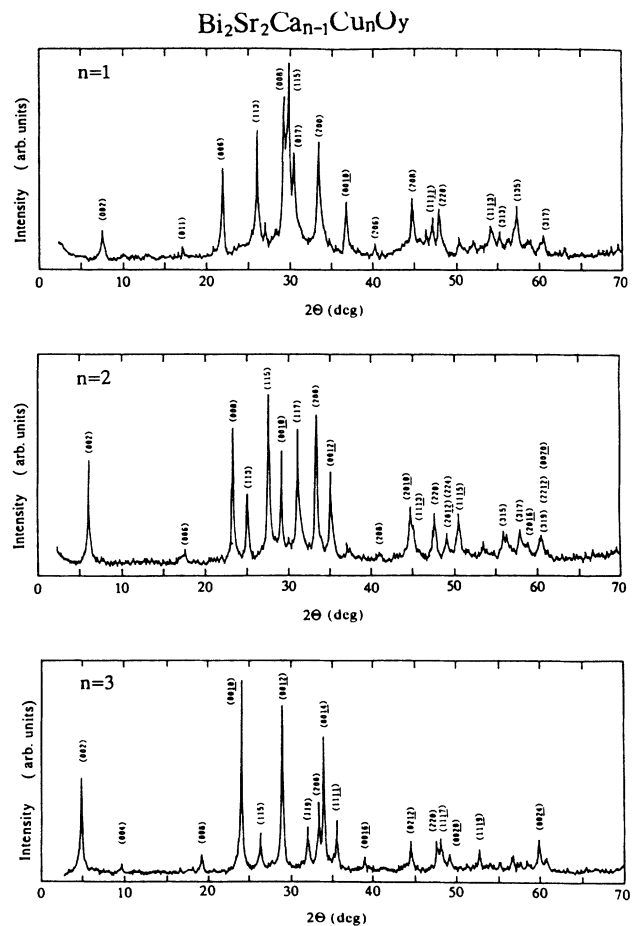


FIG. 1. Cu $K\alpha$ powder x-ray-diffraction pattern for typical single-phase samples of the $n = 1$ (2:2:0:1), $n = 2$ (2:2:1:2), and $n = 3$ (2:2:2:3) samples. Nominal compositions are $\text{Bi}_{2.1}\text{Sr}_{1.9}\text{CuO}_y$, $\text{Bi}_2\text{Sr}_{1.8}\text{Ca}_{1.2}\text{Cu}_2\text{O}_y$, and $\text{Bi}_{1.85}\text{Pb}_{0.35}\text{Sr}_2\text{Ca}_2\text{Cu}_{3.1}\text{O}_y$, respectively.

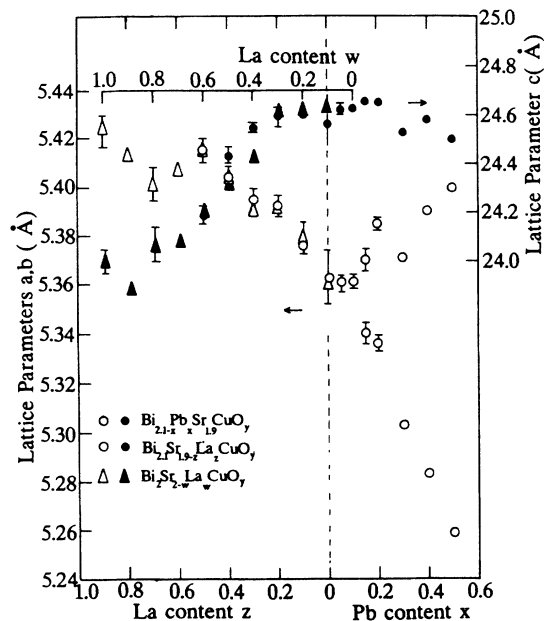


FIG. 2. Lattice constants of La- and Pb-doped 2:2:0:1 samples (series B, C, and D). For convenience, for two series of La-doped samples, the abscissa is displaced in order that the sum of the valences of Bi (assumed to be trivalent), Sr, and La becomes equal.

Figure 4 shows the lattice parameters of Y-doped and Pb-doped 2:2:1:2 samples. A single-phase sample was synthesized for $0 \leq x \leq 0.6$ for Y doping and for $0 \leq z \leq 0.2$ for Pb doping. Recently, Fukushima *et al.* succeeded in obtaining Pb-doped samples up to $z = 0.3$ by sintering under the reduced atmosphere.³⁶ In our experiment, sintering was performed in air. Thus, the samples with x larger than 0.2 always contain other phases. In the case of Y doping, the c parameter decrease with increasing x , whereas the a parameter increases with increasing Y content. The tetragonal to orthorhombic transition can be observed at around $x = 0.6$. These features were almost the same as those obtained by Tamegai *et al.*²¹ Although the $x = 1.0$ sample is not sin-

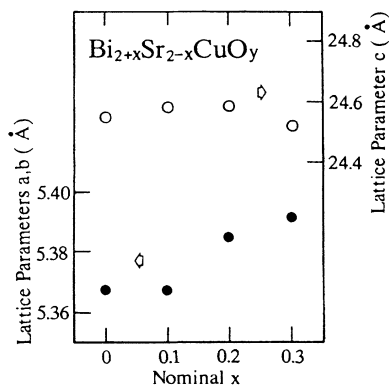


FIG. 3. Lattice constants of $\text{Bi}_{2+x}\text{Sr}_{2-x}\text{CuO}_y$ samples.

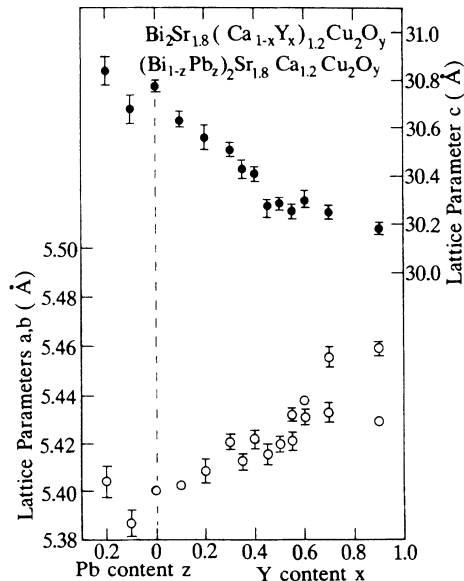


FIG. 4. Lattice constants of Y- and Pb-doped 2:2:1:2 samples (series E and F).

gle phase, similar magnitudes of the lattice parameters were obtained for single crystals of $\text{Bi}_2\text{Sr}_2\text{YO}_y$ prepared by a CuO flux method.³⁷

Figure 5 shows the schematic phase diagram of the 2:2:2:3 sample prepared from the nominal composition of $\text{Bi}_{1.85}\text{Pb}_{0.3}(\text{Sr}_{1-x}\text{Ca}_x)_4\text{Cu}_{3.1}\text{O}_y$. Single-phase 2:2:2:3 samples can be obtained only for the narrow range of the nominal composition (black region in this figure). If we plot the lattice constants for 2:2:2:3 samples including those obtained in other regions, there was very little dependence of a , b , and c on x . This strongly suggests the lack of flexibility of the 2:2:2:3 structure. In the 2:2:2:3 structure, we have not succeeded in substituting other cations yet. This may be due to the rigidity of this structure mentioned just above.

Figure 6 shows examples of the thermogravimetric (TG) curves of various samples of the Bi systems. For every sample, the change in oxygen content with increasing temperature is about 0.8 weight % at maximum, and below 600 °C there is almost no loss of oxygen. The maximum change in oxygen content deduced from the data in Fig. 6 is 0.06, 0.05, and 0.03 for the unit formula of the

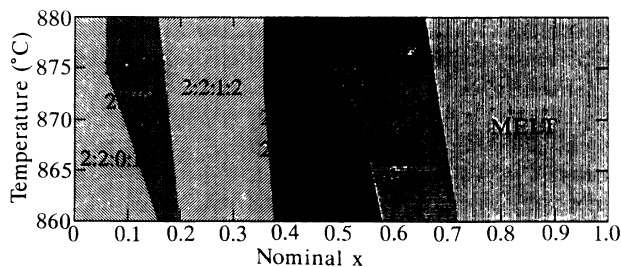


FIG. 5. Summary of the relation between the preparation conditions (nominal composition and the sintering temperature) and the prepared phases of $\text{Bi}_{1.85}\text{Pb}_{0.3}(\text{Sr}_{1-x}\text{Ca}_x)_4\text{Cu}_{3.1}\text{O}_y$.

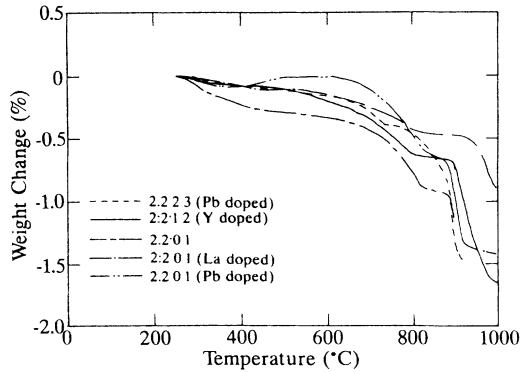


FIG. 6. Thermogravimetric curves for various samples of Bi compounds. Nominal compositions are $\text{Bi}_{2.1}\text{Sr}_{1.9}\text{CuO}_y$ (nondoped 2:2:0:1), $\text{Bi}_2\text{Sr}_{1.6}\text{La}_{0.4}\text{CuO}_y$ (La-doped 2:2:0:1), $\text{Bi}_{1.8}\text{Pb}_{0.3}\text{Sr}_{1.9}\text{CuO}_y$ (Pb-doped 2:2:0:1), $\text{Bi}_2\text{Sr}_{1.8}\text{Ca}_{0.96}\text{Y}_{0.24}\text{Cu}_2\text{O}_y$ (Y-doped 2:2:1:2), and $\text{Bi}_{1.85}\text{Pb}_{0.35}\text{Sr}_2\text{Ca}_2\text{Cu}_3\text{O}_y$ (2:2:2:3), respectively.

2:2:0:1, 2:2:1:2, and 2:2:2:3 phases, respectively. Thus, as far as oxygen deficiency during heat cycles is concerned, the Bi system has less oxygen deficiency than the 1:2:3 compounds. This is probably due to the absence of the chain structure in this compound.

Figures 7–9 show the average valence of Cu for La-doped 2:2:0:1, Pb-doped 2:2:0:1, and Y-doped 2:2:1:2 samples, respectively. In the case of La doping and Y doping, the average valence of Cu decreases with increasing La or Y content. On the other hand, the Pb doping increases the average valence of Cu very little. In the following equations we simply assume that Pb is divalent and Bi is trivalent, and denote the average valence of Cu as $2+p$, the oxygen content $6+\delta$ and $8+\delta$ for 2:2:0:1 and 2:2:1:2 samples, respectively. Then, p is represented as

$$p = 2\delta - w \quad \text{for } \text{Bi}_2\text{Sr}_{2-w}\text{La}_w\text{CuO}_y, \quad (1)$$

$$p = 2\delta + x - 0.1 \quad \text{for } \text{Bi}_{2.1-x}\text{Pb}_x\text{Sr}_{1.9}\text{CuO}_y, \quad (2)$$

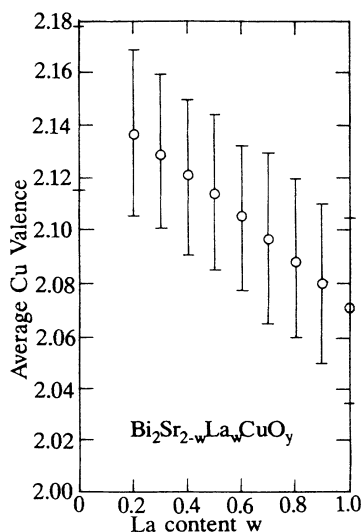


FIG. 7. Average Cu valence of $\text{Bi}_2\text{Sr}_{2-w}\text{La}_w\text{CuO}_y$ determined by the iodometric titration method.

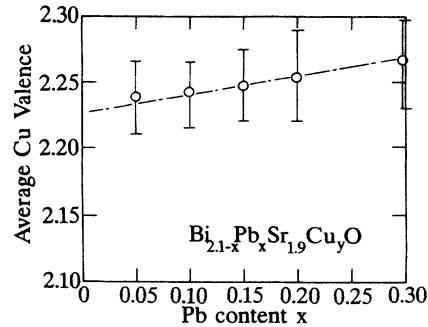


FIG. 8. Average Cu valence of $\text{Bi}_{2.1-x}\text{Pb}_x\text{Sr}_{1.9}\text{CuO}_y$ determined by the iodometric titration method.

$$p = \delta - 0.6x \quad \text{for } \text{Bi}_2\text{Sr}_{1.8}(\text{Ca}_{1-x}\text{Y}_x)_{1.2}\text{Cu}_2\text{O}_y. \quad (3)$$

We should note that the observed change in the average valence of Cu is much less than expected from the above equations assuming that δ does not change. Thus, the origin of this discrepancy should be ascribed to the change of δ by changing the concentration of the substituting cations. In fact, the increase of oxygen content was reported in La-doped 2:2:1:2 samples by several groups.^{25,38}

In nondoped 2:2:0:1 materials, we performed the titration only for $\text{Bi}_{2.1}\text{Sr}_{1.9}\text{CuO}_y$, which was found to have the average valence of 2.14. However, Ikeda *et al.*³⁵ obtained the average Cu valence in $\text{Bi}_{2+x}\text{Sr}_{2-x}\text{CuO}_y$ series materials by measuring the oxygen content. According to their result, the valence was found to be almost constant (around 2.15) up to $x=0.15-0.20$, and decreases with increasing x .

For Pb-doped 2:2:1:2 samples, p of 0.21 and 0.30 were obtained for $z=0.1$ and 0.2, respectively.

For 2:2:2:3 samples, the obtained p is about 0.15 for every sample, if we assume carriers are doped in two CuO_2 layers.

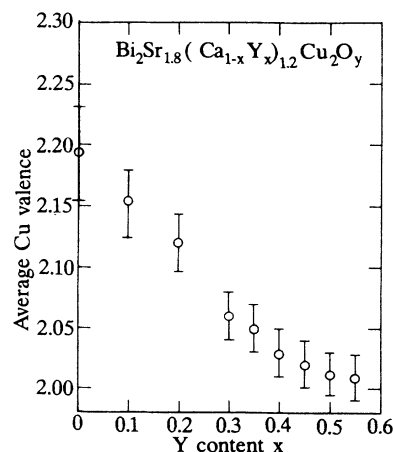


FIG. 9. Average Cu valence of $\text{Bi}_2\text{Sr}_{1.8}(\text{Ca}_{1-x}\text{Y}_x)_{1.2}\text{Cu}_2\text{O}_y$ determined by the iodometric titration method.

B. Superconductivity

1. $n=1$ (2:2:0:1) material

Figure 10 shows the temperature dependence of the resistivity for various 2:2:0:1 samples. In the case of La doping, heavily substituted samples ($w \geq 0.9$) are semiconducting. The magnitude of the resistivity decreases with increasing La content, and a transition from semiconductor to superconductor was observed at around $w=0.8$. The superconducting transition temperature T_c increases with decreasing La content and reached 25 K at $w=0.4$. In Pb-doped samples, the temperature dependence of the resistivity is metallic for the whole range of x . The resistivity decreases with increasing Pb content up to $x=0.3$. With additional increasing Pb content, the resistivity increases. This increase of the resistivity is probably due to the existence of the impurity phase, which became observable even in powder x-ray diffraction pattern at $x=0.6$. T_c decreases with increasing Pb content. At $x=0.3$, only the onset temperature was observed.

Figure 11(a) shows the Meissner effect of La-doped 2:2:0:1 samples. Although at lowest temperatures, the diamagnetic signal is large enough to guarantee the bulk superconductivity, the diamagnetic signal above 18 K, for instance in the $w=0.4$ sample, is very small, which leads one to suspect that the onset temperature of the

bulk superconductivity is lower than 25 K. However, we should note that the temperature dependence of the susceptibility shows downward concave behavior. This is similar to that reported by Muller *et al.* in the 2:1:4 material.³⁹ Thus, we can assume that the bulk superconductivity surely occurs at 25 K. In fact, the diamagnetic susceptibility measured under a lower magnetic field is larger than that shown in Fig. 11(a). We also investigate Nd-doped 2:2:0:1 samples, which also display a large diamagnetic signal at around 20 K. Thus, we can rule out the possibility of the superconductivity due to the 2:1:4 material. As was previously mentioned, the La doping based on $\text{Bi}_{2.1}\text{Sr}_{1.9}\text{CuO}_y$ was also performed (series B). In this case, the diamagnetic signal was very small (5×10^{-4} emu/g at most). Thus, measurement of the physical properties were performed only in the $\text{Bi}_2\text{Sr}_{2-w}\text{La}_w\text{CuO}_y$ samples (series C).

Figure 11(b) shows the Meissner effect in Pb-doped 2:2:0:1 samples. Although it clearly shows that the superconductivity is due to the 2:2:0:1 phase, the bulk superconductivity disappears at $x=0.2$. The dependence of T_c as a function of the nominal composition w and x and z is summarized in Fig. 12. With increasing La content, the system undergoes a superconductor-to-semiconductor transition. On the other hand, with increasing Pb content, the system undergoes another superconductor-to-nonsuperconductor transition. Thus, together with the results in Figs. 7 and 8, the following

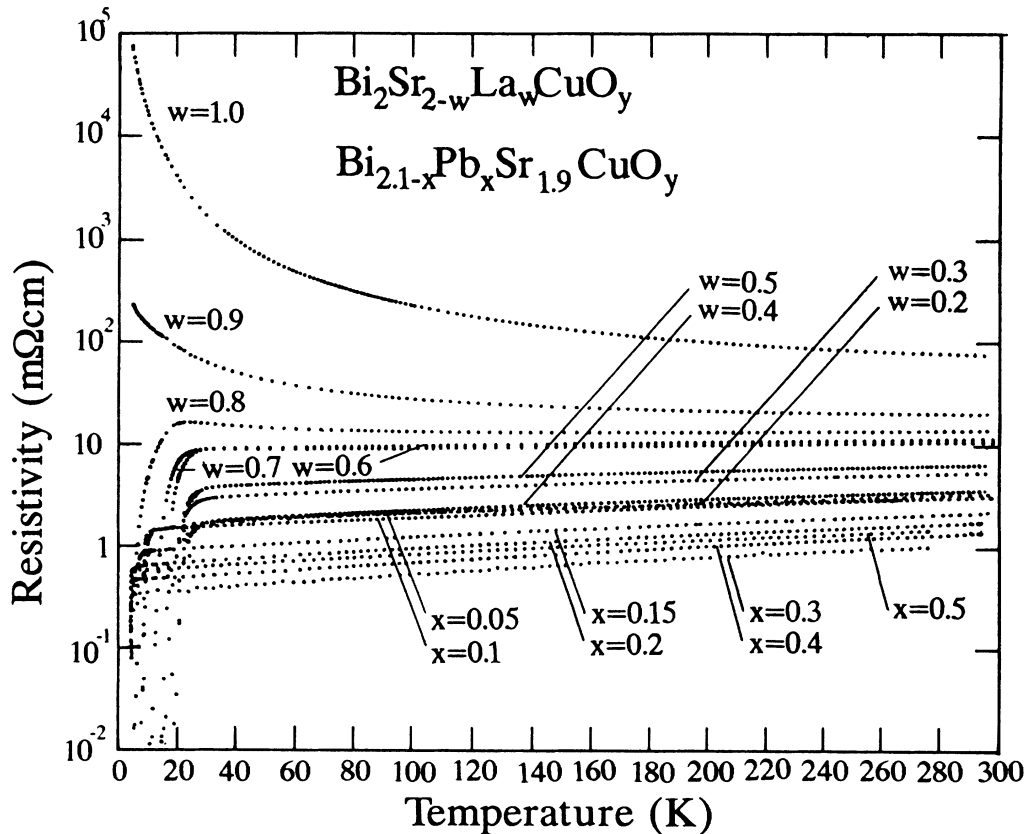


FIG. 10. Temperature dependence of the resistivity of La- and Pb-doped 2:2:0:1 samples (series C and D).

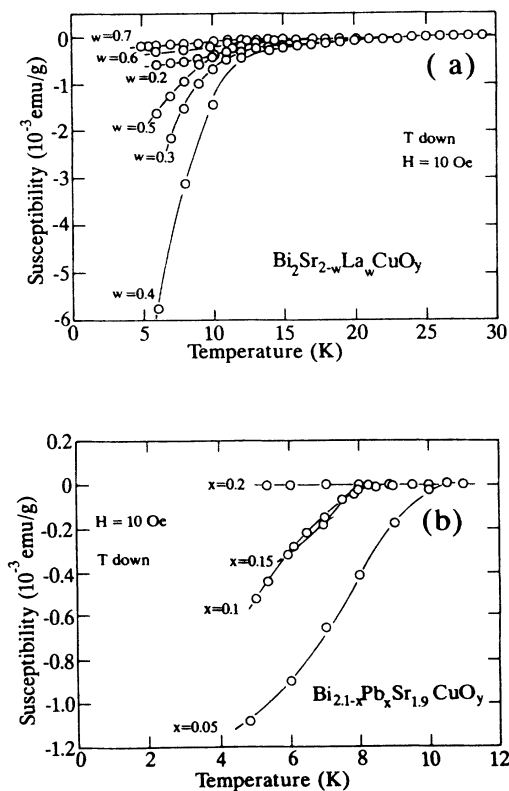


FIG. 11. Meissner effect of 2:2:0:1 samples measured with decreasing temperature under the magnetic field of 10 Oe: (a) $\text{Bi}_2\text{Sr}_{1-w}\text{La}_w\text{CuO}_y$ (series C); (b) $\text{Bi}_{2.1-x}\text{Pb}_x\text{Sr}_{1.9}\text{CuO}_y$ (series D).

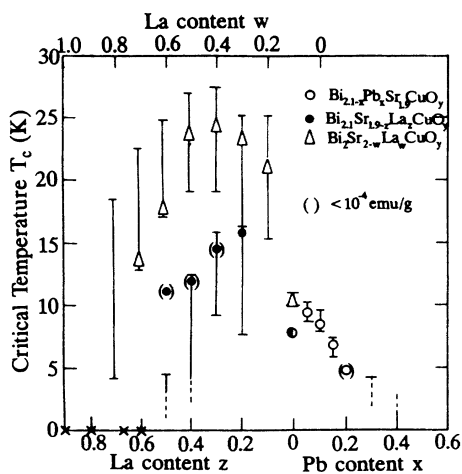


FIG. 12. Superconducting transition temperature of 2:2:0:1 samples as a function of a nominal concentration of La or Pb. For convenience, for two series of La-doped samples the abscissa is displaced in order that the total valence of Bi (assumed to be trivalent), Sr, and La becomes equal. Bars show the onset and zero-resistance temperatures determined by resistivity measurement; circles, triangles, and squares show T_c determined by Meissner effect measurement. Brackets represent that the Meissner signal is smaller than 10^{-4} emu/g. \times 's represent that the material does not show the superconducting transition temperature.

features were revealed in the 2:2:0:1 materials: With an increasing mean valence of Cu, the magnitude of the resistivity decreases monotonically whereas T_c increases, and after taking a maximum, T_c decreases when further increasing the average valence of Cu, and finally bulk superconductivity disappears.

It should be also noted that the T -linear dependence of the resistivity is observed in La-doped superconducting samples. On the other hand Pb-doped samples exhibit the concave downward behavior like normal metals.³⁰

Even in nondoped 2:2:0:1 materials (series A), both superconducting and semiconducting samples can also be obtained by changing the ratio of Bi to Sr. Among the single-phase samples, only the sample with $x=0.1$ is a superconductor with T_c of 8 K; others are semiconducting. However, the magnitude of the Meissner effect is less than 3% of the complete Meissner effect at most.

2. $n=2$ (2:2:1:2) material

Figure 13 shows the temperature dependence of the resistivity for various 2:2:1:2 samples. By the doping of Y, first the superconducting transition temperature T_c increases with increasing Y content up to 0.1, and decreases with further increasing Y content. Finally it becomes semiconducting. Thus, a superconductor-semiconductor transition was observed at $x=0.45$. However, a feature different from 2:2:0:1 samples is evident, i.e., a two-step transition was observed for superconducting samples with x larger than 0.1, which was also reported by other groups.^{21,22} The two-step transition was also observed in the Meissner effect shown in Fig. 14. For a higher- T_c transition, no hysteresis for the heat cycle was observed. If we plot T_c as shown in Fig. 15, the higher T_c would then be found to be unchanged with increasing Y content, whereas the lower T_c decreases with decreasing temperature. Thus, a most natural interpretation of the dependence of T_c on the Y content is that there exist two different 2:2:1:2 phases with two different Y contents. We can roughly estimate the lower limit of the superconducting volume fraction from the Meissner data. The estimated lower limit of the volume fraction of the higher- T_c 2:2:1:2 phase is about 5%. On the other hand, we cannot find any sign of the phase separation into a different 2:2:1:2 phase with a different Y content in the powder x-ray diffraction pattern. In the Bi compounds, it often occurs that the diamagnetic signal is quite large though the x-ray powder pattern does not show the existence of the corresponding superconducting phase.²⁷ Thus, the actual volume fraction of the higher- T_c 2:2:1:2 phase seems to be small. Thus, the existence of the higher- T_c 2:2:1:2 phase is considered not to affect the estimation of the Cu valence and other physical properties substantially. Therefore, we will regard the lower T_c as that of the material with given nominal composition.

In Pb-doped samples, T_c was decreased down to 60 K. In this case, the superconducting transition was very sharp, as shown in Fig. 14.

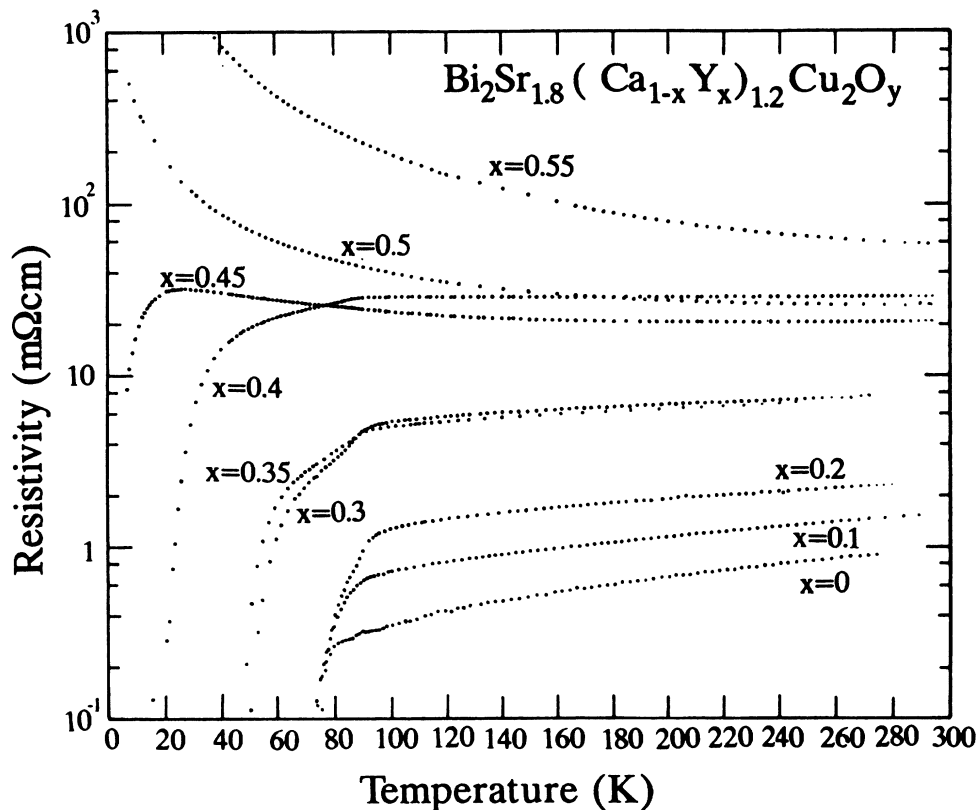


FIG. 13. Temperature dependence of resistivity for Y-doped 2:2:1:2 samples (series E).

3. $n = 3$ (2:2:2:3) material

Figure 16 shows the temperature dependence of the resistivity of a single-phase 2:2:2:3 sample. The “as-sintered” sample (sample A) shows a small tail around 110 K and the resistivity at room temperature is relatively high (4 mΩ cm). On the other hand, the Meissner effect measurement in Fig. 17 shows that the diamagnetic volume fraction is about 55% of the complete Meissner effect. As was clarified in Ref. 28, the tail observed at approximately T_c is due not to the mixing of the other phases, but due to the extremely porous nature of the as-

sintered 2:2:2:3 sample. Thus, repulverization, repressing, and resintering of the sintered pellet were necessary. The temperature dependence of the resistivity for the 2:2:2:3 samples after this additional treatment was shown also in Fig. 16. The sample after the additional treatment (sample B) shows a sharp superconducting transition with zero-resistance temperature at 107 K, and the resistivity at room temperature is about 1 mΩ cm, which is much smaller than that before the treatment. It

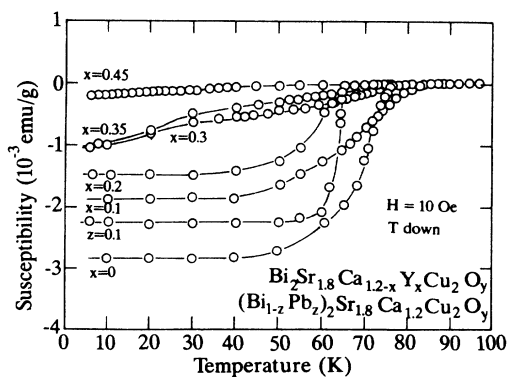


FIG. 14. Meissner effect of Y- and Pb-doped 2:2:1:2 samples (series E and F) measured with decreasing temperature under the magnetic field of 10 Oe.

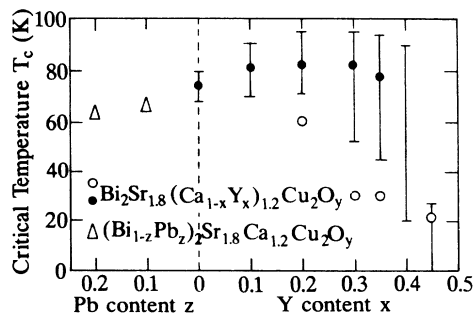


FIG. 15. Superconducting transition temperature of 2:2:1:2 samples (series E and F) as a function of the nominal concentration of Y or Pb. Bars show the onset and zero-resistance temperatures determined by resistivity measurement; circles and triangles show T_c determined by Meissner effect measurement. Two circles of the same composition for Y-doped samples with $x > 0.1$ represent two T_c 's corresponding to the two-step transition observed even in Meissner effect measurement.

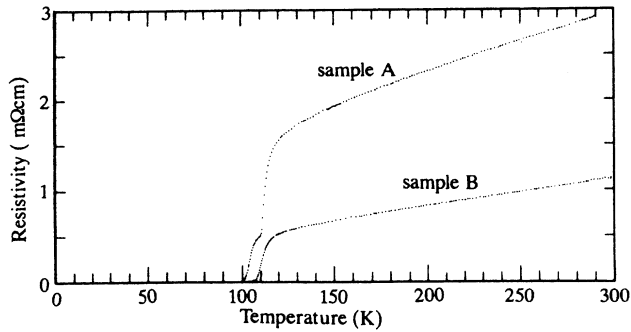


FIG. 16. Temperature dependence of the resistivity of $\text{Bi}_{1.85}\text{Pb}_{0.35}\text{Sr}_2\text{Ca}_2\text{Cu}_{3.1}\text{O}_y$ (2:2:2:3) before (sample A) and after (sample B) the treatment. Sample B was sintered at 830°C for 3 h after the repulverization.

is confirmed by the powder x-ray diffraction and the magnetic susceptibility measurement that the sample is still single phase after this treatment.

The reason for the observed change may be explained as follows. In pure 2:2:2:3 samples, the polycrystal grains were coupled ineffectively both in the normal state and in the superconducting state because of the volume expansion during the initial sintering process, even though each grain grows very well. Thus, the repulverization and resintering improves the intergrain coupling drastically. This is easily confirmed by the ac susceptibility measurement, the result of which is shown in Fig. 18. Before the treatment, the loss structure can be observed even far below T_c , and no peak was observed in the imaginary part measured at 4 Oe. On the other hand, after the treatment, a peak in the loss structure emerged at 90 K in the susceptibility measured at 4 Oe. This definitely indicates that the nature of the grain boundary is excellently improved by the heat treatment. The drastic change in

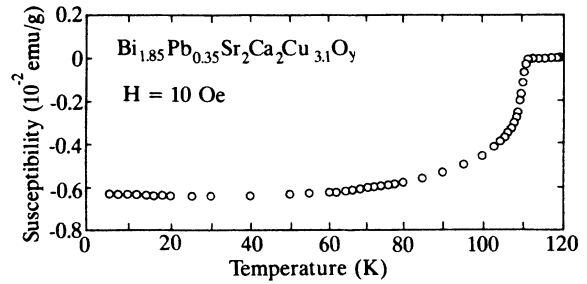


FIG. 17. Meissner effect of $\text{Bi}_{1.85}\text{Pb}_{0.35}\text{Sr}_2\text{Ca}_2\text{Cu}_{3.1}\text{O}_y$ measured with decreasing temperature under the presence of a magnetic field of 10 Oe.

the morphology was also confirmed by the SEM-EPMA measurement.⁴⁰ It will be shown that this improvement has an essential effect for the measurement of the Hall coefficient.

It should also be noted that the samples with sharp superconducting transition and relatively low resistivity can be obtained without the treatment described above—for example, if we start from the composition of $\text{Bi}_{1.85}\text{Pb}_{0.35}\text{Sr}_{2.2}\text{Ca}_{1.8}\text{Cu}_{3.1}\text{O}_y$ (Fig. 19). However, as is shown in the inset, this sample contains almost an equal amount of the 2:2:1:2 phase and the 2:2:2:3 phase. These samples cannot be used for the measurement of the physical properties.

4. The transition temperature as a function of the hole concentration

From the previously mentioned results above, it becomes possible to plot the superconducting transition temperature T_c as a function of the hole concentration. Both in the 2:2:0:1 and the 2:2:1:2 materials, the materials are superconducting when the average valence of Cu

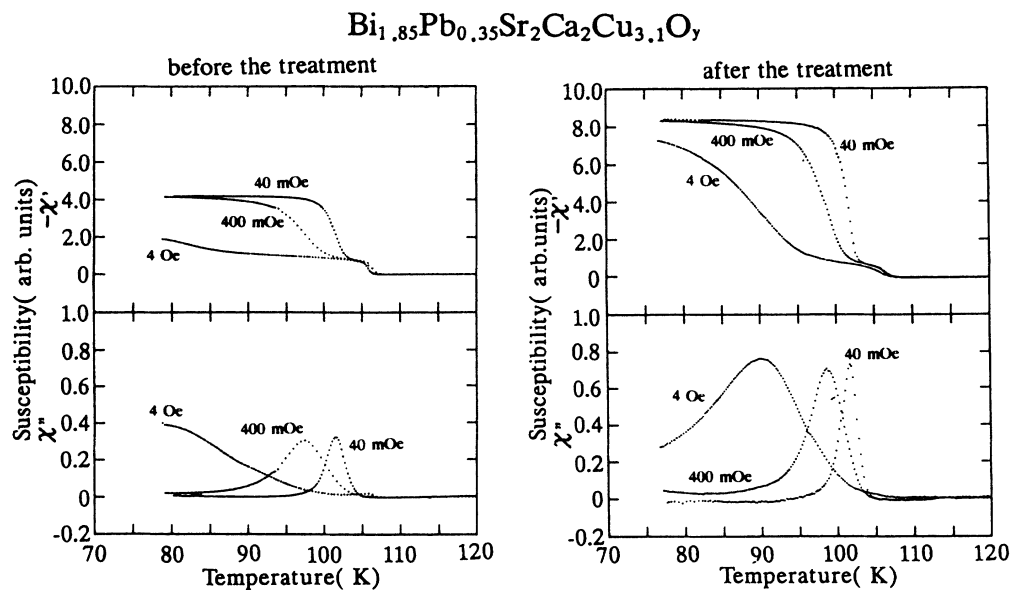


FIG. 18. Complex susceptibility $\chi = \chi' - i\chi''$ of $\text{Bi}_{1.85}\text{Pb}_{0.35}\text{Sr}_2\text{Ca}_2\text{Cu}_{3.1}\text{O}_y$ before and after the treatment. The frequency of the alternating magnetic field is 2 kHz, and the amplitude is 40 mOe, 400 mOe, and 4 Oe.

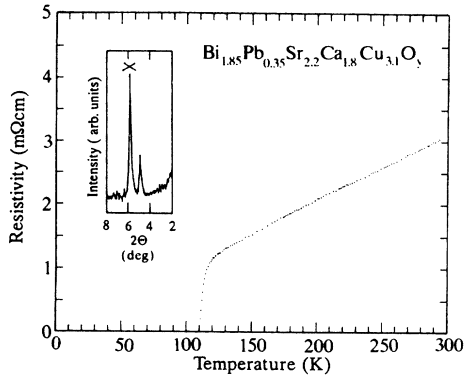


FIG. 19. An example of a mixed-phase 2:2:2:3 sample which shows a sharp resistive transition and low resistivity. The inset shows the powder x-ray diffraction pattern of the same sample. \times indicates the peak of the 2:2:2:3 phase.

is large, and become semiconducting when the average valence of Cu decreases and approaches 2. Thus, we can also consider in the Bi compounds that the material with the average valence of Cu of 2.0, which corresponds exactly to the d^9 configuration, is a Mott insulator without any free carriers. Then, we can regard the deviation of the average Cu valence from a value of 2 as the hole concentration.

Figure 20 shows T_c as a function of the hole concentration p for the 2:2:0:1, the 2:2:1:2, and the 2:2:2:3 materials. In the 2:2:0:1 system, the material became superconducting at $p=0.09$, and T_c increases with increasing p . With further increasing p , T_c decreases after assuming a maximum value of 25 K of approximately $p=0.12$. Finally the bulk superconductivity disappears at around $p=0.25$. This behavior is similar to that observed in the (La,Sr)-Cu-O system.^{2,12}

For nondoped 2:2:0:1 materials (series A), the obtained

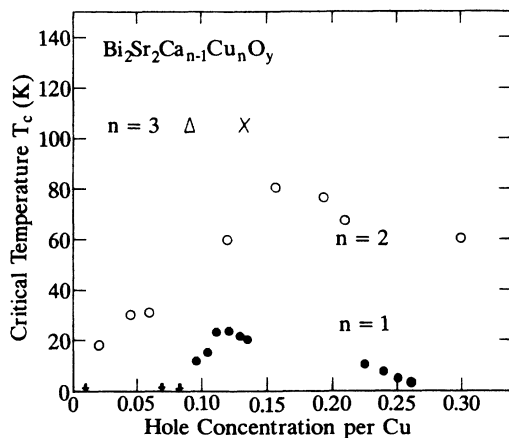


FIG. 20. Superconducting transition temperature T_c as a function of the hole concentration for the 2:2:0:1 (series C and D), 2:2:1:2 (series E and F), and 2:2:2:3 (series G) samples. Δ and \times for the 2:2:2:3 materials represent the points obtained under the assumption that holes are distributed with equal probability in three and two CuO_2 layers, respectively. Arrows indicate that the materials are semiconducting.

result is slightly different from those in La-doped 2:2:0:1 materials (series C). If we plot the point for the superconductor $\text{Bi}_{2.1}\text{Sr}_{1.9}\text{CuO}_y$ in the same figure (not plotted), the points do not locate on the curves obtained for La-doped samples. As will be discussed in Sec. IV B, in nondoped samples other factors are considered to influence T_c .

In the 2:2:1:2 system, the material became superconducting at $p=0.01-0.02$, and T_c increases with increasing p . With further increasing p , T_c decreases after taking a broad plateau at around $p=0.15-0.20$. In this case, we have not found the disappearance of superconductivity for large p . These behaviors are also similar to those observed in the 1:2:3 compounds.¹³

In the 2:2:2:3 system only one point was obtained. In Fig. 20, two points were plotted, and Δ and \times represent the points obtained under the assumption that holes are distributed with equal probability in three or two CuO_2 layers, respectively. Although there is little difference whether this material should be regarded as double layered or triple layered, the obtained point is not located on the T_c - p curves of the 2:2:1:2 material in both cases. Thus, it is likely that a different curve exists for the 2:2:2:3 material.

C. Normal-state properties

1. Hall effect

Figure 21 shows the temperature dependence of the Hall coefficient R_H of nondoped 2:2:0:1, 2:2:1:2, and 2:2:2:3 samples. Among superconducting nondoped 2:2:0:1 samples and semiconducting 2:2:0:1 samples we could not find any definite difference in the magnitude and the temperature dependence of R_H . For every sample, R_H is positive, and increases with decreasing temperature. Figure 22 shows the inverse of R_H of the same samples as a function of temperature. Only the 2:2:2:3 samples showed $1/T$ dependence of the R_H . On the other hand, the 2:2:0:1 and the 2:2:1:2 sample showed much weaker temperature dependence.

Figure 23 shows the R_H as a function of the hole concentration determined in Figs. 7–9 for the 2:2:0:1 and the 2:2:1:2 materials. The dashed curves in the figure represent the inverse of e times the hole density per unit volume) where e is the electronic charge, as was originally proposed by Ong *et al.*¹⁵ As is shown in Fig. 23(a), in

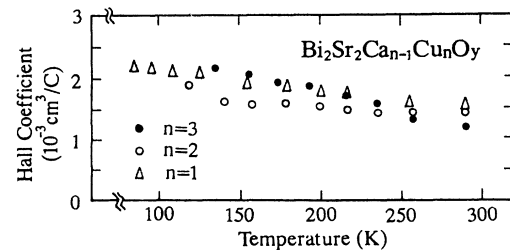


FIG. 21. Temperature dependence of the Hall coefficient R_H of $\text{Bi}_{2.1}\text{Sr}_{1.9}\text{CuO}_y$, $\text{Bi}_2(\text{Sr}_{0.6}\text{Ca}_{0.4})_3\text{Cu}_2\text{O}_y$, and $\text{Bi}_{1.85}\text{Pb}_{0.35}\text{Sr}_2\text{Ca}_2\text{Cu}_{3.1}\text{O}_y$.

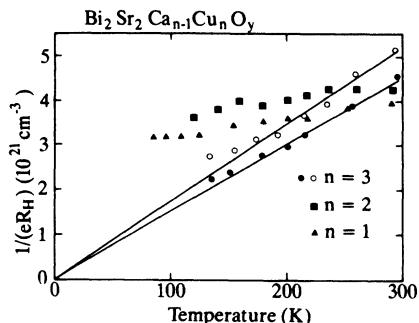


FIG. 22. Inverse of the Hall coefficient divided by the electronic charge ($1/eR_H$) of the same samples as were shown in Fig. 21 as a function of temperature. For $n=3$ (2:2:2:3) material, the data obtained in another sample were added as closed circles.

the 2:2:0:1 system, R_H is almost the same as the inverse of the hole concentration at small hole concentrations. It strongly deviates from the inverse of the hole concentration with increasing hole concentration. The hole concentration where the deviation starts to occur roughly corresponds to the hole concentration where semiconductor-to-superconductor transition occurs. On the other hand, in the 2:2:1:2 system, apart from the difference of the absolute magnitude, R_H roughly scales with the inverse of hole concentration up to high-hole concentration where T_c begins to decrease with increasing hole concentration.

For the 2:2:2:3 sample, as was reported previously,²⁸ the Hall coefficient decreases to half by the additional treatment. The final value of R_H ; $1 \times 10^{-3} \text{ cm}^3/\text{C}$ corresponds to the hole concentration per Cu of 0.47. Clayhold *et al.* obtained a much smaller value of the Hall number $1/eR_H$ in the early stage.⁴¹ Judging from the temperature dependence of the resistivity of their sam-

ples, we think this is probably due to the low quality of the grain boundaries of their sample.

2. Infrared reflection

Figure 24 shows the infrared reflection spectra of non-doped 2:2:0:1, 2:2:1:2, and 2:2:2:3 samples. The absolute value of the reflectivity at 4000 cm^{-1} is 24% (2:2:0:1), 35% (2:2:1:2), and 45% (2:2:2:3). It looks like the plasma reflection of free electrons. Edge structure definitely moves to a higher energy with an increasing number of CuO_2 layers. For an additional step, the fitting to the Drude-type formula is desirable. Although the absolute magnitude of the reflectivity strongly depends on the condition of the polished polycrystals, the data in Fig. 24 show a relatively large value of reflectivity. Thus, the data in Fig. 24 were fitted tentatively to the ordinary Drude formula without any correction. The determined "plasma frequencies" were 5500 cm^{-1} (2:2:0:1), 7400 cm^{-1} (2:2:1:2), and 8800 cm^{-1} (2:2:2:3), which are indicated by arrows in the figure. The obtained characteristic frequency increases with increasing n .

All the data in Fig. 24 were taken for polycrystals. It is necessary to check whether there is an essential difference between the "plasma frequencies" of polycrystals and that of single crystals. Figure 25 shows the comparison of the reflection spectra of 2:2:1:2 materials between a polycrystal and a highly oriented film prepared by the molecular beam epitaxy MBE method. The polycrystal shows a slightly smaller value of the characteristic frequency. Thus, the measurement with polycrystalline samples has a meaning only in qualitative comparison.

Figure 26 shows the infrared reflection spectra of various 2:2:1:2 samples with different hole concentrations. In this figure, for comparison, the minimum value of the reflectivity is equated to 8%. The edge frequency does not move with the change of hole concentration and T_c ,

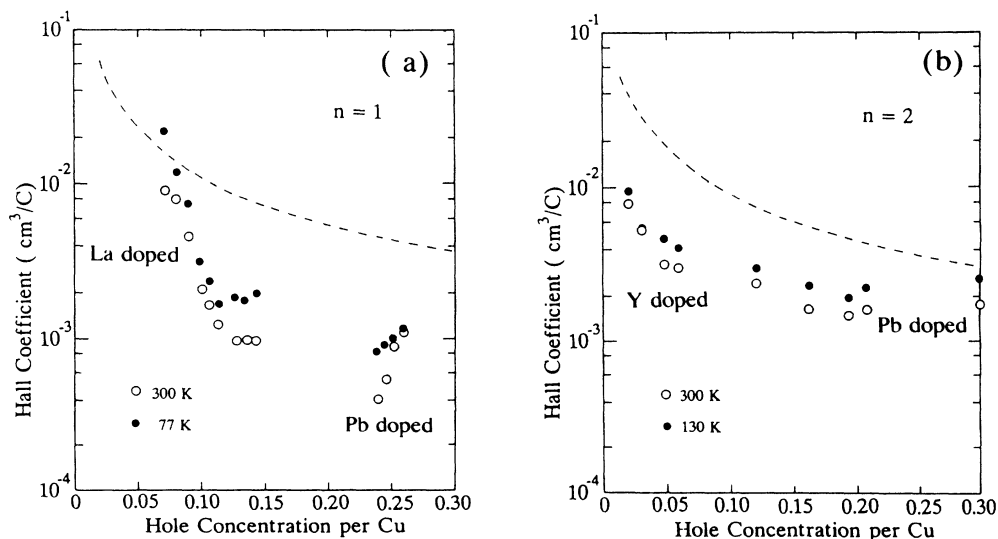


FIG. 23. Hall coefficients as a function of the hole concentration determined by the titration for (a) 2:2:0:1 samples (series C and D), and for (b) 2:2:1:2 samples (series E and F). Dashed curves shown in the figures represent the inverse of the hole concentration p per unit volume multiplied by the electronic charge ($1/ep$).

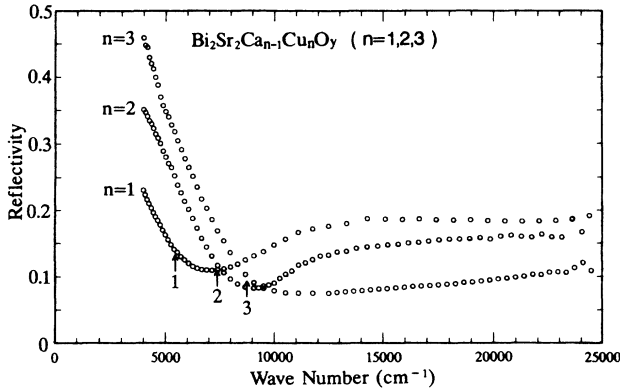


FIG. 24. Infrared-visible optical reflection spectra for $\text{Bi}_{2.1}\text{Sr}_{1.9}\text{CuO}_y$ (2:2:0:1), $\text{Bi}_2\text{Sr}_{1.8}\text{Ca}_{1.2}\text{Cu}_2\text{O}_y$ (2:2:1:2), and $\text{Bi}_{1.85}\text{Pb}_{0.35}\text{Sr}_2\text{Ca}_2\text{Cu}_{3.1}\text{O}_y$ (2:2:2:3). Arrows indicate the “plasma frequency” obtained by the fitting to an ordinary Drude formula.

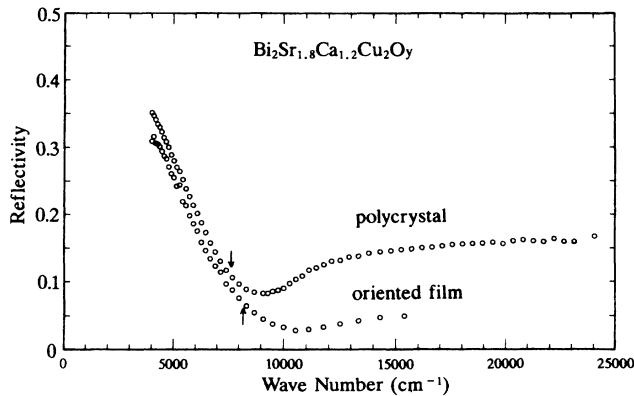


FIG. 25. Infrared-visible optical reflection spectra of the 2:2:1:2 material: (a) A polycrystal with the nominal composition of $\text{Bi}_2\text{Sr}_{1.8}\text{Ca}_{1.2}\text{Cu}_2\text{O}_y$; (b) an oriented film made by coevaporation. Arrows indicate the “plasma frequency” obtained by the fitting to ordinary Drude formula.

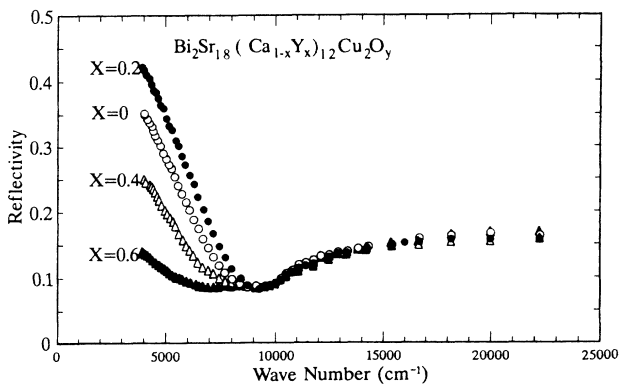


FIG. 26. Infrared-visible optical reflection spectra of Y-doped 2:2:1:2 polycrystals ($\text{Bi}_2\text{Sr}_{1.8}(\text{Ca}_{1-x}\text{Y}_x)_{1.2}\text{Cu}_2\text{O}_y$) with $x=0, 0.2, 0.4$, and 0.6 . For comparison, the data for all samples were plotted as the minimum reflectivity is equal to 8%. The true minimum reflectivities of the samples are 7.49% ($x=0$), 6.33% ($x=0.2$), 8.33% ($x=0.4$), and 7.38% ($x=0.6$).

which is different from the behavior observed in Fig. 24. A similar behavior was observed in 2:2:0:1 samples, as is shown in Fig. 27. Thus, within the same structure, namely the same number of CuO_2 sheets n , the edge frequency was found not to change although the superconducting transition temperature T_c changes. This is very similar to the behavior of “plasma frequency” observed in (La,Sr)-Cu-O system.^{17,18}

For the nondoped 2:2:0:1 materials (series A), the obtained reflection spectra are almost the same between a superconducting sample and a semiconducting sample.

3. Magnetic susceptibility

Figure 28 shows the magnetic susceptibility of 2:2:0:1 materials with a different hole concentration. In La-doped samples, the susceptibility has very weak temperature dependence. For samples with small hole concentration, the measured susceptibility is negative. Considering that the core diamagnetic contribution is -2.3×10^{-7} emu/g, the remaining paramagnetic contribution is 1.5×10^{-7} emu/g at 300 K. For the samples with high hole concentration (Pb-doped ones), the magnitude of the susceptibility is larger, and the temperature dependence is Curie-like.

In a semiconducting sample, a small hump can be observed at around 280 K. Figure 29 shows the result of the more detailed measurement in an expanded scale. The susceptibility assumes a local maximum at 280 K, which is similar to the temperature dependence of the susceptibility of (La,Sr)-Cu-O.⁴² This strongly suggests that the antiferromagnetic transition occurs at this temperature. Although we have not performed any other magnetic measurement, this structure should be regarded as due to the antiferromagnetic transition. To our knowledge, this is the first time that the antiferromagnetic transition was observed in static susceptibility in Bi compounds. We have not observed similar transitions within the measured temperature range in other samples

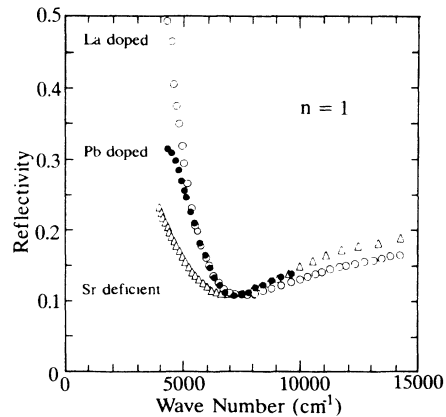


FIG. 27. Infrared-visible optical reflection spectra of La-doped ($\text{Bi}_2\text{Sr}_{1.6}\text{La}_{0.4}\text{CuO}_y$), Pb-doped ($\text{Bi}_{1.8}\text{Pb}_{0.3}\text{Sr}_{1.9}\text{CuO}_y$), and nondoped ($\text{Bi}_{2.1}\text{Sr}_{1.9}\text{CuO}_y$) 2:2:0:1 polycrystals. For comparison, the data for all samples were plotted as the minimum reflectivity is equal to 10%. The true minimum reflectivities of the samples are 10% (the nondoped-Sr deficient sample), 7.5% (the La-doped sample), and 3% (the Pb-doped sample).

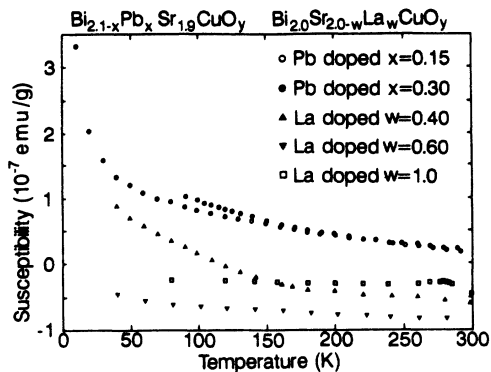


FIG. 28. Temperature dependence of the magnetic susceptibility of La- and Pb-doped 2:2:0:1 materials (series C and D) with $x=0.15$ and 0.30 and $w=0.40, 0.60$, and 1.0 . The magnitude of the magnetic field was 5 kOe.

with different compositions.

In the nondoped 2:2:0:1 (series A) samples, the susceptibility is weakly Curielike for all samples. No definite change was found when the ratio of Bi to Sr was changed.

For the 2:2:1:2 materials, the behavior of the measured susceptibility is essentially the same as reported in Ref. 21.

Figure 30 shows the temperature dependence of the susceptibility of a 2:2:2:3 sample. It shows a very broad peak around 170 K. This behavior is observed in several samples.

IV. DISCUSSION

A. On the structural properties

In the Bi-Sr-Ca-Cu-O system, the existence of the complicated modulated structure^{4,43-45} has made the precise structural analysis almost impossible. Very recently, Yamamoto *et al.*⁴⁶ succeeded in performing the Rietveld refinement of the neutron-diffraction data including those of modulated structure in a nondoped 2:2:1:2 polycrystalline sample. According to their analysis, even Cu atoms and oxygen atoms in the CuO_2 layer are displaced sub-

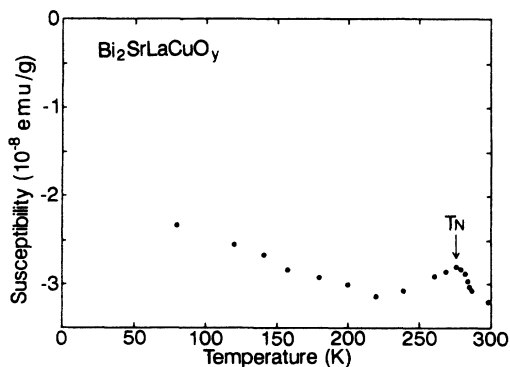


FIG. 29. Temperature dependence of the magnetic susceptibility of $\text{Bi}_2\text{SrLaCuO}_y$ in an expanded scale. T_N indicating the peak represents the temperature where antiferromagnetic order is considered to be formed.

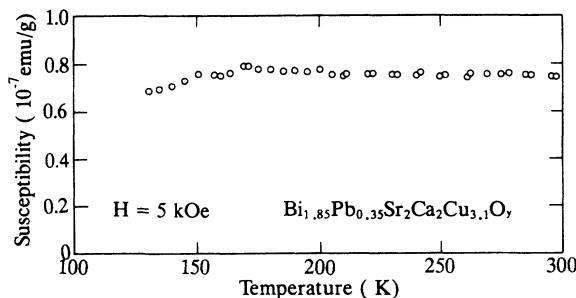


FIG. 30. Temperature dependence of the magnetic susceptibility of $\text{Bi}_{1.85}\text{Pb}_{0.35}\text{Sr}_2\text{Ca}_2\text{Cu}_{3.1}\text{O}_y$. The applied magnetic field was 5 kOe.

stantially from their average positions due to the existence of the modulated structure in the Bi_2O_2 plane. Thus, from the structural point of view the existence of the modulated structure is expected to affect the physical properties strongly. The period of the modulated structure changes by the doping of La to the 2:2:0:1 materials³⁸ or Y to the 2:2:1:2 materials.²¹ In Pb-doped 2:2:0:1 and 2:2:1:2 samples, the modulated structure changes drastically by the slight doping, and the further doping eliminates the modulated structure completely.^{36,47} At present, the effect of the modulated structure on the physical properties is not known. However, in Pb-doped samples, as was shown in Fig. 10, the disappearance of the modulated structure did not induce sudden change in T_c or resistivity. Thus, it seems that the existence of the modulated structure does not affect the physical properties so much. For further consideration, detailed study on the Cu—O bond length for various samples are needed.

B. On the relation between T_c and hole concentration

As was shown in Fig. 20, the semiconductor-superconductor-normal metal transition with increasing hole concentration was also found in the Bi 2:2:0:1 phase. The 2:2:1:2 phase also displays the semiconductor-superconductor transition, and T_c decreases after showing saturation in the high hole-concentration region. From the magnetic susceptibility measurement shown in Fig. 29, the semiconducting phase in the 2:2:0:1 phase was found to be an antiferromagnetic insulator. For the 2:2:1:2 phase, the antiferromagnetic ordering was already confirmed by the muon spin-relaxation (μSR) experiment. Thus, also in Bi compounds, the superconductivity is considered to occur by doping a hole in the Mott-Hubbard insulator with antiferromagnetic ordering. Considering that the similar phase diagrams were obtained in the 2:1:4 and the 1:2:3 compounds, the antiferromagnetic insulator-superconductor-normal metal transition with increasing hole concentration was found to be quite a general feature in copper-oxide based high- T_c superconductors. However, the result in Fig. 20 clearly shows that the three different curves exist for materials with different n . Thus, although the mechanism of high- T_c superconductivity must be the same among single-, double-, and triple-layered materials, it seems that some

extra factor(s) should be taken into account in double- or triple-layered material in order to explain the superconductivity above liquid-nitrogen temperature. In this sense, the single-layered TI material which shows T_c of 90 K is very interesting.^{6,48} The reason why the 90 K superconductivity is possible with only one CuO_2 layer will be clarified soon.

We should also discuss the origin of holes in undoped Bi-Sr-Cu-Cu-O systems where sufficient holes already exist. According to the structure refinement by Yamamoto *et al.*,⁴⁶ excess oxygen atoms ($\delta=1.0$) exist in the Bi-dilute region of Bi_2O_2 layers, which is consistent with crystallochemical considerations by Ikeda *et al.*³⁵ Thus, the most dominant origin of the hole reservoir in undoped materials is the excess oxygen existing in the Bi_2O_2 layers. The deficiency of Sr or Ca may also provide holes. However, they are likely to be the secondary candidate.

A puzzling phenomenon is that of the semiconductor-to-superconductor transition observed in nondoped 2:2:0:1 materials (series A). The measured hole concentration was not different between superconducting samples and semiconducting samples (see Sec. III C 1). Furthermore, other physical properties (R_H , optical reflection, susceptibility, etc.) are almost the same between these samples. Thus, in order to explain this phenomenon, other factors like randomness should be taken into account. In fact, in the 2:2:1:2 samples doped with Fe, Co, Ni, and Zn T_c decreases with increasing impurity concentration without changing hole concentration.⁴⁹

C. Hall effect

The above results show that the electric conduction in these materials is positive-hole conduction. For the 2:2:0:1 materials, in the small-hole-concentration region R_H coincides well with the inverse of the hole concentration. This is consistent with the picture of the existence of only one kind of hole doped in a Mott-Hubbard split band. However, with increasing hole concentration, R_H strongly deviates from the inverse of the hole concentration and superconductivity occurs in the concentration range where this deviation becomes clear. Thus, it may be said that the appearance of the high- T_c superconductivity strongly correlates with the destruction of the Mott-Hubbard character of electronic structure, as was suggested by Takagi *et al.* in the 2:1:4 system.⁵⁰ However, in the 2:2:1:2 materials, apart from the difference in absolute magnitude, R_H scales well with the inverse of hole concentration even in the high-hole concentration region. This suggests that the Mott-Hubbard character of the electronic structure still survives even in the concentration range where superconductivity above liquid-nitrogen temperature occurs. A similar result was obtained in the 1:2:3 systems, as was already described in Sec. I. Thus, from these results, we may say that in single-layered systems R_H strongly deviates from the inverse of hole concentration with increasing hole concentration, whereas in double-layered systems both scale very well up to the high-hole concentration region.

In general, the Hall coefficient is a complicated func-

tion of the shape of the Fermi surface.⁵¹ Thus, a detailed calculation is necessary for determining the sign and the magnitude of R_H . In almost all the high- T_c oxides, however, the R_H is positive, which is understood by the simple picture of a single-band hole injected into a filled band formed by Mott-Hubbard splitting. These holes cause superconductivity. The observed dependence of R_H on the hole concentration in the single-layered materials suggests that the band structure itself changes by the doping. In fact, the change in electronic structure was observed in transmission spectra of single crystalline films in the (La,Sr)-Cu-O system.¹⁸ On the other hand, the observed dependence of R_H on the hole concentration in the double-layered materials suggests that the rigid-band picture holds well even for the hole concentration where high- T_c superconductivity occurs. Thus, the change in band structure by the doping, namely the destruction of the Mott-Hubbard splitting may not be essential to the high- T_c superconductivity. Another possible interpretation is that in the double-layered systems high- T_c superconductivity is possible even in the Mott-Hubbard split band due to some extra factor which is absent in single-layered materials, interlayer coupling, and so on. Yoshizaki *et al.*⁵² also observed the scaling behavior of R_H and the inverse of the hole concentration in the Bi-Sr-Ca-Cu-O 2:2:1:2 system, and proposed that the difference of the effective mass is the possible origin of the difference discussed above. The difference in the coordination number of Cu among these materials may also be another possible origin. Anyway, detailed measurement of the electronic structure of low-energy excitation in single crystals is needed for further discussion.

It should be also noted that the magnitude of R_H in 2:2:1:2 systems differ from the inverse of the hole concentration by a factor of 2, although the scaling relation holds well. Clayhold *et al.*⁵³ suggested that the deficiency in Sr or Bi may be the origin of this discrepancy, because their estimation of the hole concentration was made by the estimation of the charge balance from the known oxygen content. In our case, we estimated the hole concentration directly from the titration technique. Thus, the deficiency of the cations cannot be the origin of the discrepancy. The simplest solution is to assume the coexistence of electron and hole.⁵¹ Band-structure calculations for this system^{54,55} show the existence of two bands crossing the Fermi level: one has CuO character and the other has BiO character. However, experimentally, Bi_2O_2 layers were found to be insulating.⁵⁶ Thus, the possibility of the coexistence of a hole and electron is ruled out. Another possible origin is the large anisotropy of the Bi-Sr-Ca-Cu-O system. The Bi compounds have large anisotropy in normal-state properties. Thus, the Hall coefficient measured in polycrystalline samples may differ substantially from the true value. In other cuprate superconductors, in spite of the existence of the anisotropy, R_H measured in polycrystalline samples is almost the same as or only slightly smaller than that measured in single crystals. However, in the case of the Bi-Sr-Ca-Cu-O 2:2:1:2 system, R_H measured in a single crystal⁵⁷ is closer to the dashed curve in Fig. 23. Thus, anisotropy may be one possible origin of the difference.

Most puzzling is the temperature dependence of the Hall coefficient. The $1/T$ law has been suggested for the 1:2:3 compounds.^{2,58} However, as is easily understood from Fig. 22, the $1/T$ law is only valid for the 2:2:2:3 material in the Bi systems. Thus, the $1/T$ law does not seem to be a common feature of high- T_c oxides. Anyway, the temperature-dependent Hall coefficient in this system should be correlated with anomalous features in the normal state of high- T_c oxides.⁵⁸ Together with the temperature dependence of the resistivity, the anomalous temperature dependence of R_H should be understood soon.

D. Optical reflection spectra

As was shown in Figs. 24–27, a definite structure exists in the optical reflection spectra of mid-infrared to visible regions. This kind of structure has been interpreted as the plasma reflection of free carriers.^{17,18} In fact, the data taken in a single crystal of the 2:2:1:2 phase fit well to the ordinary Drude formula.⁵⁷ However, in the (La,Sr)-Cu-O system the obtained plasma frequency which should be proportional to the square root of the carrier density does not change with increasing hole concentration.^{17,18} The same feature was found in our experiment on the Bi compounds shown in Figs. 26 and 27. On the other hand, a μ SR experiment by Uemura *et al.*⁵⁹ shows that the relaxation rate of the muon which should be proportional to the plasma frequency surely increases with increasing hole concentration. Thus, the most natural explanation for this discrepancy is to regard the “plasma reflection” observed in optical spectra as the contribution from quite different origins. In fact, the strong deviation from the Drude behavior was reported in low-frequency regions in the 1:2:3 system.¹⁹ Very recently, the detailed measurement by Watanabe *et al.*⁶⁰ revealed that the reflectivity in single crystals of the 1:2:3 compounds even in the infrared-to-visible region does not fit to the Drude formula well.

Several models have been presented on the interpretation of the optical reflection spectra based on the interband transition.^{61,62} Tachiki *et al.*⁶³ showed theoretically that new levels appear in the charge transfer gap as a result of the many-body effect, which may also bring about anomalous optical spectra. Anyway, the optical spectrum in this frequency region should be discussed with that in lower and higher frequency regions, simultaneously. In fact, the intensity of the charge-transfer absorption observed in semiconducting samples decreases gradually by the doping of the carrier, and the “Drude” structure increases at the same time.⁶⁴ Thus, the analysis taking account of only the charge transfer absorption or the “Drude” structure seems to be insufficient. Detailed analyses based on the data taken in single crystals are now in progress.

E. Magnetic susceptibility

The broad peak observed in $\text{Bi}_2\text{SrLaCuO}_y$ shown in Fig. 29 demonstrates that the semiconducting phase in the low-hole-concentration region is an antiferromagnetic insulator. Around this hole-concentration region, the

temperature dependence of the susceptibility is very weak. With increasing hole concentration, the temperature dependence of the susceptibility becomes Curielike, and the magnitude of the susceptibility increases.

For the 2:2:2:3 materials, the temperature dependence of the susceptibility is also very weak, and a broad hump exists at around 170 K.

At present, there are two different directions on the interpretation of the magnetic susceptibility in high- T_c oxides. One is that the magnetic susceptibility is due to the ordinary Pauli paramagnetic susceptibility due to free electrons.⁶⁵ The other is that the large paramagnetic susceptibility is due to the spin fluctuation characteristic to two-dimensional systems.^{50,66}

In the former interpretation, we can estimate the density of states at the Fermi level $N(0)$ from the susceptibility data. For instance, if we take χ^{spin} (300 K) = 1.5×10^{-7} emu/g, $N(0)$ of 3 states/Cu spin is obtained for $\text{Bi}_2\text{Sr}_{1.6}\text{La}_{0.4}\text{CuO}_y$. However, even semiconducting material has a large paramagnetic component of the same order of magnitude which contradicts the interpretation due to the Pauli paramagnetism. Many other properties measured demonstrate that these materials are a very strongly correlated system.² Furthermore, the complicated temperature dependence seems hard to be explained in terms of the ordinary Pauli paramagnetism. In fact, a nuclear magnetic resonance (NMR) experiment showed that a large antiferromagnetic correlation exists between Cu and O.⁶⁷ Thus, it seems that the paramagnetic susceptibility in these materials should be regarded as due to the antiferromagnetic fluctuation of spins.

Here it should be noted that in Pb-doped samples the susceptibility is more Curielike than in La-doped samples. On the other hand, the resistivity becomes lower with increasing Pb content. If the Curielike component is due to the existence of impurity phases, resistivity should increase with increasing Curie component. A similar increase of the Curie component was reported also in the (La,Sr)-Cu-O system,⁵⁰ which was interpreted as the destruction of the spin fluctuation of Cu directly observed in the neutron-diffraction experiment.⁶⁸ The curious temperature dependence of the susceptibility in the 2:2:2:3 sample should be interpreted also in terms of the spin fluctuation. In fact, the temperature dependence of T_1^{-1} in the NMR experiment was not found to obey a Korringa relation.⁶⁹ These have been interpreted as the decrease of the spin excitation,⁷⁰ which is in good agreement with the result of neutron diffraction.⁷¹

From these arguments, the magnetic susceptibility in this system should be understood in terms of the spin fluctuation under the presence of antiferromagnetic correlation.

V. CONCLUSION

Polycrystalline samples of $\text{Bi}_2\text{Sr}_2\text{Ca}_{n-1}\text{Cu}_n\text{O}_y$ with various hole concentrations were synthesized by substituting La for Sr, Y for Ca, and Pb for Bi. After characterization, superconducting properties, normal-state properties (the magnetic susceptibilities, Hall coefficient, and infrared optical reflection spectra) were investigated.

For $n=1$ materials, the antiferromagnetic semiconductor-superconductor-normal metal transition was observed with increasing hole concentration. In other systems, the relation between T_c and the hole concentration was found to have different curves, although the basic feature was the same. Thus, although the mechanism of superconductivity is the same among these materials, some extra factor seems to play an important role in double- and triple-layered materials. This was also derived from the Hall-coefficient measurement. The "Drudelike" structure was observed in the infrared-to-visible region. From the comparison among samples with different hole concentration and different n , the origin of this structure was considered to be quite different from the plasma reflection. The large paramagnetic susceptibility was found to have a complex temperature dependence. All of the observed behaviors in the resistivity, Hall coefficient, the optical reflection spectrum, and the magnetic susceptibility are far from those expected in ordinary Fermi-liquid theory. Thus, the physical properties including superconductivity in the Bi-Sr-Ca-Cu-O system should be described in terms of the strongly correlated

spin-charge systems. To date, relatively few theories treating such systems have been developed. Additional developments in this area are eagerly awaited.

ACKNOWLEDGMENTS

We thank Professor N. P. Ong of Princeton University, Professor K. Kishio and I. Terasaki of the University of Tokyo, Dr. S. Tajima of International Superconducting Technology Center (ISTEC), Professor R. Yoshizaki, and Professor K. Takita of Tsukuba University, Dr. Y. Matsui of the National Institute for Research in Inorganic Materials for stimulating discussions, A. Fukuoka and Professor K. Kitazawa of the University of Tokyo for SEM-EPMA measurements, and Y. Nakayama of the University of Tokyo for providing us the thin films. We also thank Y. Kato, T. Shibauchi, Y. Nakajima, and H. Watanabe of the University of Tokyo for their technical assistance. This work was partially supported by a Grant-in-Aid for Specially Promoted Research on High-Temperature Superconductors (No. 62065004) from the Ministry of Education, Science, and Culture of Japan.

- ¹J. G. Bednorz and K. A. Muller, *Z. Phys. B* **64**, 189 (1986).
- ²For a review, for example, *Physical Properties of High Temperature Superconductors*, edited by D. M. Ginsberg (World-Scientific, Singapore, 1988).
- ³C. Michel, M. Hervieu, M. M. Borel, A. Gradin, F. Deslandes, J. Provost, and B. Raveau, *Z. Phys. B* **68**, 421 (1987).
- ⁴J. Akimitsu, A. Yamazaki, H. Sawa, and H. Fujiki, *Jpn. J. Appl. Phys.* **26**, L2080 (1987).
- ⁵H. Maeda, T. Tanaka, M. Fukutomi, and T. Asano, *Jpn. J. Appl. Phys.* **27**, L209 (1988).
- ⁶Z. Z. Sheng and A. M. Hermann, *Nature*, **332**, 55 (1988).
- ⁷R. M. Hazen, L. W. Finger, R. J. Angel, C. T. Prewitt, N. L. Ross, C. G. Hadjidakos, P. J. Heaney, D. R. Veblen, Z. Z. Sheng, A. El Ali, and A. M. Hermann, *Phys. Rev. Lett.* **60**, 1657 (1988).
- ⁸J. M. Tarascon, Y. Le Page, P. Barboux, B. G. Bagley, L. H. Greene, M. R. McKinnon, G. W. Hull, M. Giroud, and D. M. Hwang, *Phys. Rev. B* **37**, 9382 (1988).
- ⁹E. Takayama-Muromachi, Y. Uchida, A. Ono, F. Izumi, M. Onoda, Y. Matsui, K. Kosuda, S. Takekawa, and K. Kato, *Jpn. J. Appl. Phys.* **27**, L365 (1988); E. Takayama-Muromachi, Y. Uchida, Y. Matsui, M. Onoda, and K. Kato, *ibid.* **27**, L556 (1988).
- ¹⁰M. A. Subramanian, C. C. Torardi, J. C. Calabrese, J. Gopalakrishnan, K. J. Morrissey, T. R. Askew, R. B. Flippen, U. Chowdhry, and A. W. Sleight, *Science*, **239**, 1015 (1988).
- ¹¹H. Ihara, R. Sugise, M. Hirabayashi, N. Terada, M. Jo, K. Hayashi, A. Negishi, M. Tokumoto, Y. Kimura, and T. Shimomura, *Nature* **334**, 510 (1988).
- ¹²J. B. Torrance, Y. Tokura, A. I. Nazzal, A. Bezing, T. C. Huang, and S. S. Parkin, *Phys. Rev. Lett.* **61**, 1127 (1988).
- ¹³Y. Tokura, J. B. Torrance, T. C. Huang, and A. I. Nazzal, *Phys. Rev. B* **38**, 7156 (1988).
- ¹⁴S. Uchida, H. Takagi, H. Ishii, H. Eisaki, T. Yabe, S. Tajima, and S. Tanaka, *Jpn. J. Appl. Phys.* **26**, L440 (1987).
- ¹⁵N. P. Ong, Z. Z. Wang, J. Clayhold, J. M. Tarascon, L. H. Greene, and W. R. McKinnon, *Phys. Rev. B* **35**, 8807 (1987).
- ¹⁶K. Takita, H. Akinaga, K. Masuda, H. Asano, Y. Takeda, M. Takano, K. Nishiyama, and K. Nagamine, in *Proceedings of the Tsukuba Seminar on High- T_c Superconductivity*, Tsukuba, 1989, edited by K. Masuda, T. Arai, I. Iguchi, and R. Yoshizaki (University of Tsukuba, Tsukuba, 1989), p. 11.
- ¹⁷S. Tajima, T. Nakahashi, S. Uchida, and S. Tanaka, *Physica* **156C**, 90 (1988).
- ¹⁸M. Suzuki, *Phys. Rev. B* **39**, 2312 (1989).
- ¹⁹G. A. Thomas, J. Orenstein, D. H. Rapkine, M. Capizzi, A. J. Millis, R. N. Bhatt, L. F. Schneemeyer, and J. V. Waszczak, *Phys. Rev. Lett.* **61**, 1313 (1988).
- ²⁰N. Fukushima, H. Niu, and K. Ando, *Jpn. J. Appl. Phys.* **27**, L790 (1988); *ibid.* **27**, L1432 (1988).
- ²¹T. Tamegai, A. Watanabe, K. Koga, I. Oguro, and Y. Iye, *Jpn. J. Appl. Phys.* **27**, L1074 (1988).
- ²²Y. Koike, Y. Iwabuchi, S. Hosoya, N. Kobayashi, and T. Fukase, *Physica* **C159**, 105 (1989).
- ²³J. M. Tarascon, P. Barboux, G. W. Hull, R. Ramesh, H. H. Greene, M. Giroud, M. S. Hedge, and W. R. McKinnon, *Phys. Rev. B* **39**, 4316 (1989).
- ²⁴M. Onoda, M. Sera, K. Fukuda, S. Kondoh, M. Sato, T. Den, H. Sawa, and J. Akimitsu, *Solid State Commun.* **66**, 189 (1988); T. Den, A. Yamazaki, and J. Akimitsu, *Jpn. J. Appl. Phys.* **27**, L1620 (1988).
- ²⁵T. Kijima, J. Tanaka, and Y. Bando, *Jpn. J. Appl. Phys.* **27**, L1035 (1988).
- ²⁶Y. Takemura, M. Hongo, and S. Yamazaki, *Jpn. J. Appl. Phys.* **28**, L916 (1989).
- ²⁷A. Maeda, T. Yabe, H. Ikuta, Y. Nakayama, T. Wada, S. Okuda, T. Itoh, M. Izumi, K. Uchinokura, S. Uchida, and S. Tanaka, *Jpn. J. Appl. Phys.* **27**, L661 (1988).
- ²⁸A. Maeda, K. Noda, K. Uchinokura, and S. Tanaka, *Jpn. J. Appl. Phys.* **28**, L576 (1989).
- ²⁹A. Maeda, K. Noda, S. Takebayashi, and K. Uchinokura, *Physica* **162-164C**, 1205 (1989).
- ³⁰A. Maeda, Y. Kato, T. Shibauchi, Y. Nakajima, H. Watanabe,

- and K. Uchinokura, *Jpn. J. Appl. Phys.* **28**, L1549 (1989).
- ³¹M. Takano, J. Takada, K. Oda, H. Kitaguchi, Y. Miura, Y. Ikeda, Y. Tomii, and H. Mazaki, *Jpn. J. Appl. Phys.* **27**, L1041 (1988).
- ³²U. Endo, S. Koyama, and T. Kawai, *Jpn. J. Appl. Phys.* **27**, L1476 (1988).
- ³³T. Hatano, K. Aota, S. Ikeda, K. Nakamura, and K. Ogawa, *Jpn. J. Appl. Phys.* **27**, L2055 (1988).
- ³⁴Y. Matsui, A. Maeda, K. Uchinokura, and S. Takekawa, *Jpn. J. Appl. Phys.* (to be published).
- ³⁵Y. Ikeda, H. Ito, S. Shimomura, Y. Oue, K. Inaba, Z. Hiroi, and M. Takano, *Physica* **159C**, 93 (1989).
- ³⁶N. Fukushima, H. Niu, S. Nakamura, S. Takeno, M. Hayashi, and K. Ando, *Physica* **159C**, 777 (1989).
- ³⁷S. Takebayashi, T. Nakahashi, I. Terasaki, A. Maeda, K. Uchinokura (unpublished).
- ³⁸W. Bauhofer, H. J. Mattausch, R. K. Tremer, P. Murugaraj, and A. Simon, *Phys. Rev. B* **39**, 7244 (1989).
- ³⁹K. A. Muller, M. Takashige, and J. G. Bednorz, *Phys. Rev. Lett.* **58**, 1143 (1987).
- ⁴⁰A. Maeda, K. Noda, S. Takebayashi, K. Uchinokura, A. Fukuoka, and K. Kitazawa (unpublished).
- ⁴¹J. C. Clayhold, N. P. Ong, P. H. Hor, and C. W. Chu, *Phys. Rev. B* **38**, 7016 (1988).
- ⁴²K. K. Singh, P. Ganguly, and J. B. Goodenough, *J. Solid State Chem.* **52**, 254 (1984); N. Nguyen, F. Studer, and B. Raveau, *J. Phys. Chem. Solids* **44**, 389 (1983); H. Takagi, S. Uchida, H. Obara, K. Kishio, K. Kitazawa, K. Fueki, and S. Tanaka, *Jpn. J. Appl. Phys.* **26**, L434 (1987).
- ⁴³Y. Matsui, S. Takekawa, S. Horiuchi, and A. Umezono, *Jpn. J. Appl. Phys.* **27**, L1873 (1988).
- ⁴⁴Y. Matsui, S. Takekawa, H. Nazaki, and A. Umezono, *Jpn. J. Appl. Phys.* **28**, L602 (1989).
- ⁴⁵S. Ikeda, K. Aota, T. Hatano, and K. Ogawa, *Jpn. J. Appl. Phys.* **27**, L2040 (1988).
- ⁴⁶A. Yamamoto, M. Onoda, E. Takayama-Muromachi, F. Izumi, T. Ishigaki, and H. Asano (unpublished).
- ⁴⁷Y. Matsui (private communication).
- ⁴⁸Y. Kubo, Y. Shimakawa, T. Manako, T. Satoh, S. Iijima, T. Ichihashi, and H. Igarashi, *Physica* **162-164C**, 991 (1989).
- ⁴⁹K. Uchinokura, T. Yabe, S. Takebayashi, M. Hase, and A. Maeda, *Physica* **162-164C**, 981 (1981); *Phys. Rev. B* **41**, 4118 (1990).
- ⁵⁰H. Takagi, T. Ido, S. Ishibashi, M. Uota, S. Uchida, and Y. Tokura, *Phys. Rev. B* **40**, 2254 (1989).
- ⁵¹J. M. Ziman, *Principles of the Theory of Solids* (Cambridge University Press, Cambridge, 1972), p. 248.
- ⁵²R. Yoshizaki, H. Kurahashi, N. Ishikawa, M. Akamatsu, J. Fujikami, and H. Ikeda, in *Proceedings of the Tsukuba Seminar on High- T_c Superconductivity*, Tsukuba, 1989, edited by K. Masuda, T. Arai, I. Iguchi, and R. Yoshizaki (University of Tsukuba, Tsukuba, 1989), p. 21.
- ⁵³J. Clayhold, S. J. Hagen, N. P. Ong, J. M. Tarascon, and P. Barboux, *Phys. Rev. B* **39**, 7320 (1989).
- ⁵⁴L. F. Mattheiss and D. R. Hamann, *Phys. Rev. B* **38**, 5012 (1988).
- ⁵⁵F. Herman, R. V. Kasovski, and W. Y. Hsu, *Phys. Rev. B* **38**, 204 (1988).
- ⁵⁶H. Yoshida, T. Takahashi, Y. Okabe, H. Mori, X. Wang, S. Yamada, and Y. Endoh (unpublished).
- ⁵⁷H. Takagi, H. Eisaki, S. Uchida, A. Maeda, S. Tajima, K. Uchinokura, and S. Uchida, *Nature* **332**, 236 (1988).
- ⁵⁸J. Clayhold, N. P. Ong, Z. Z. Wang, J. M. Tarascon, and P. Barboux, *Phys. Rev. B* **39**, 7324 (1989).
- ⁵⁹Y. J. Uemura *et al.*, *Phys. Rev. Lett.* **62**, 2317 (1989).
- ⁶⁰Y. Watanabe, Z. Z. Wang, S. A. Lyon, D. C. Tsui, N. P. Ong, J. M. Tarascon, and P. Barboux, *Phys. Rev. B* **40**, 6884 (1989).
- ⁶¹S. Etamad, D. E. Aspnes, M. K. Kelly, R. Thompson, J. M. Tarascon, and G. W. Hull, *Phys. Rev. B* **37**, 3396 (1988).
- ⁶²T. Arima, H. Nobumasa, K. Shimomura, and T. Kawai, *Jpn. J. Appl. Phys.* **28**, L913 (1989).
- ⁶³M. Tachiki and S. Takahashi, *Phys. Rev. B* **38**, 218 (1988); **39**, 293 (1989).
- ⁶⁴S. Tajima (unpublished).
- ⁶⁵See for example, G. Grüner, *Physica* **162-164C**, 8 (1989).
- ⁶⁶H. A. Algra, L. J. de Jongh, and R. L. Carlin, *Physica* **93B**, 24 (1978).
- ⁶⁷M. Takigawa, P. C. Hammel, R. H. Heffner, Z. Fisk, K. C. Ott, and J. D. Thompson, *Phys. Rev. Lett.* **63**, 1865 (1989).
- ⁶⁸R. J. Birgenau, D. R. Gabbe, H. P. Jenssen, M. A. Kanster, P. J. Picore, T. R. Thurston, G. Shirane, Y. Endoh, M. Stoh, K. Yamada, Y. Hidaka, M. Oda, Y. Enomoto, M. Suzuki, and T. Murakami, *Phys. Rev. B* **37**, 7443 (1988).
- ⁶⁹K. Fujiwara, Y. Kitaoka, K. Asayama, H. Sasakura, S. Minamigawa, K. Nakahigashi, S. Nakanishi, M. Kogachi, N. Fukuoka, and Y. Yanase, *J. Phys. Soc. Jpn.* **58**, 380 (1989).
- ⁷⁰T. Imai, H. Yasuoka, T. Shimizu, Y. Ueda, and K. Kosuge, *J. Phys. Soc. Jpn.* **58**, 1528 (1989); T. Imai and H. Yasuoka, *Parity* **4**, 41 (1989).
- ⁷¹G. Shirane, R. J. Birgenau, Y. Endoh, P. Gehring, M. A. Kanster, K. Kitazawa, H. Kojima, I. Tanaka, T. R. Thurston, and K. Yamada, *Phys. Rev. Lett.* **63**, 330 (1989).

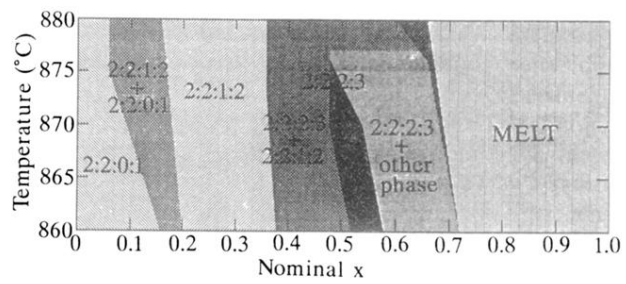


FIG. 5. Summary of the relation between the preparation conditions (nominal composition and the sintering temperature) and the prepared phases of $\text{Bi}_{1.85}\text{Pb}_{0.35}(\text{Sr}_{1-x}\text{Ca}_x)_4\text{Cu}_{3.1}\text{O}_y$.